HHS Public Access

Author manuscript

Biochemistry. Author manuscript; available in PMC 2016 October 20.

Published in final edited form as:

Biochemistry. 2015 October 20; 54(41): 6343–6351. doi:10.1021/acs.biochem.5b00816.

In-Depth Dissection of the P133R Mutation in Steroid 5β-Reductase (AKR1D1): A Molecular Basis of Bile Acid Deficiency

Mo Chen, **Yi Jin**[#], and **Trevor M. Penning**[*]

Center of Excellence in Environmental Toxicology and Department of Systems Pharmacology and Translational Therapeutics, Perelman School of Medicine University of Pennsylvania, Philadelphia, Philadelphia, United States

Abstract

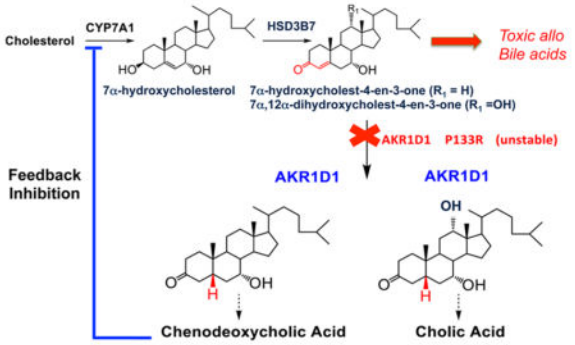

Human steroid-5β-reductase (aldo-keto reductase 1D1, AKR1D1) stereospecifically reduces Δ^4-3-ketosteroids to 5β-dihydrosteroids and is essential for steroid hormone metabolism and bile acid biosynthesis. Genetic defects in AKR1D1 cause bile acid deficiency that leads to life threatening neonatal hepatitis and cholestasis. The disease-associated P133R mutation caused significant decreases in catalytic efficiency with both the representative steroid (cortisone) and the bile acid precursor (7α-hydroxycholest-4-en-3-one) substrates. Pro133 is a second shell residue to the steroid binding channel and is distal to both the cofactor binding site and the catalytic center. Strikingly, the P133R mutation caused over a 40-fold increase in K_d values for the NADP(H) cofactors and increased the rate of release of $NADP^+$ from the enzyme by 2 orders of magnitude when compared to the wild type enzyme. By contrast the effect of the mutation on K_d values for steroids were 10-fold or less. The reduced affinity for the cofactor suggests that the mutant exists largely in the less stable cofactor-free form in the cell. Using stopped-flow spectroscopy, a significant reduction in the rate of the chemical step was observed in multiple turnover reactions catalyzed by the P133R mutant, possibly due to the altered position of NADPH. Thus, impaired

[*]Corresponding Author: Address: Department of Systems Pharmacology and Translational Therapeutics, University of Pennsylvania School of Medicine, 1315 Biochemical Research Building II/III, 421 Curie Blvd., Philadelphia, PA 19104-6160, USA. Tel.: 215-898-9445. Fax: 215-573-0200. penning@upenn.edu.

[#]Deceased: August 1, 2014.

Author Contributions

M.C. purified the proteins, performed the kinetic measurements at steady state or equilibrium, and drafted the manuscript. Y.J. performed transient kinetic measurements and revised the early drafts of the manuscript. T.M.P. supervised the overall project, was involved in data interpretation, and edited the manuscript.

The authors declare no competing financial interest.

NADPH binding and hydride transfer is the molecular basis for bile acid deficiency in patients with the P133R mutation. Results revealed that optimal cofactor binding is vulnerable to distant structural perturbation, which may apply to other disease-associated mutations in AKR1D1, all of which occur at conserved residues and are unstable.

Bile acids are amphipathic molecules that are essential for the absorption of dietary lipids and fat-soluble vitamins. All bile acids contain a steroid nucleus derived from cholesterol. Over 500 mg of cholesterol is converted to bile acids per day as an important mechanism to maintain cholesterol homeostasis.[1] Adults maintain an average bile acid pool of 2 g that recycles 12 times per day between the liver and the intestine via the enterohepatic circulation.[2] The detergent-like property of bile acids is dictated by the number and the orientation of hydroxyl groups on the steroid nucleus, but more importantly their facial amphipathicity is determined by their A/B ring *cis*-configuration which introduces a 90° bend into the steroid structure.

In humans, the A/B *cis*-configuration of bile acids is introduced by steroid-5β-reductase or aldo-keto reductase 1D1 (AKR1D1). AKR1D1 is the only known steroid 5β-reductase in humans. It is a cytosolic protein predominantly expressed in liver. It reduces all planar Δ^4-3-oxo-bile acid precursors, especially 7α-hydroxycholest-4-en-3-one and 7α, 12α-dihydroxycholest-4-en-3-one, to their mature L-shaped 5β-structures. During this reaction, the 4-pro-*R*-hydride is transferred from NADPH to the C5 of the steroid nucleus on the β-face. Without proper 5β-reduction, the less soluble Δ^4-3-oxo-bile acids accumulate which are hepatotoxic and potentially carcinogenic.[3] In addition to bile acid biosynthesis, AKR1D1 is also involved in the metabolism of all classes of steroid hormones except estrogens. 5β-Reduction mostly inactivates steroid hormones and initiates their clearance. Biologically active 5β-reduced steroids are neurosteroids[4] and tocolytic agents[5] and play roles in erythropoiesis.[6,7]

Primary bile acid deficiency is caused by inborn errors in bile acid biosynthesis, and the inherited defects in AKR1D1 were first linked to bile acid deficiency in 1988 by Setchell et al. and Clayton et al. respectively.[3,8,9] Secondary bile acid deficiency results from severe liver damage due to various diseases like hepatitis B infection and tyrosinaemia, which can result in loss of AKR1D1 expression.[10] Patients with inherited AKR1D1 deficiency often present with neonatal hepatitis and cholestatic liver disease, which might progress to life threatening cirrhosis and hepatocellular failure. Urinary sterol profiling in affected patients using mass spectrometry revealed a dramatic increase in the proportion of bile acids retaining the intermediate Δ^4-3-oxo-structure (>75%) and a significant reduction in primary bile acids (chenodeoxycholic acid and cholic acid).[8,10] An increase in the production of *allo*(5α)-bile acids is also observed presumably due to unsaturated bile acid precursors being diverted down the 5α-reductase pathway. The Δ^4-3-oxo- and *allo*-bile acids are hepatotoxic and cannot elicit the feed-back inhibition of bile acid biosynthesis at the level of *CYP7A1* expression via the farnesoid X-receptor (FXR), which results in the exacerbation of the symptoms of bile acid deficiency. Targeted disruption of the nuclear receptor FXR results in impaired lipid homeostasis resulting in increased hepatic cholesterol and triglycerides and a proatherogenic serum lipid profile suggesting that loss of its bile acid ligands could lead to

similar anomlaies.[11] AKR1D1 deficiency also results in a dramatic reduction in the 5β-metabolites of steroid hormones including both glucocorticoids and sex steroids.[12] Primary bile acid deficiency resulting from inherited AKR1D1 deficiency can be fatal in the neonate unless bile-acid supplementation is given.

Inherited AKR1D1 deficiency is an autosomal recessive disorder, which is now recognized as congenital bile acid synthesis defect type 2, CBAS 2 (OMIM 235555). Mutations in AKR1D1 were first identified in 2003 and until 2012, there were one frame-shift, two nonsense, and seven single point mutations (L106F, P133R, P198L, G223E, D241V, R261C, and R266Q) that have been identified by genetic analysis.[13–16] The seven point mutations all occur at evolutionary conserved sites,[17] and none of the residues appear to be directly involved in catalysis or ligand binding based on the crystal structure of the wild type AKR1D1.[18] Five of the mutants have been examined *in vitro* with their adverse effects on bile acid biosynthesis confirmed.[19] The mutations did not affect the transcript level of the enzyme but showed severe (L106F, P198L, G223E, and R261C) to moderate (P133R) reduction in expression levels and enzyme activity in transient transfected human embryonic kidney 293 cells.[19]

The recombinant P133R mutant was the only single point mutant that could be purified to homogeneity in *Escherichia coli* and was used as a representative for in-depth analysis of AKR1D1 associated bile acid deficiency mutations. The P133R mutation was identified in patients in a compound heterozygous status with R261C.[13] The residue is located on one of the loops capping the AKR triose-phosphate isomerase barrel on the second shell of the steroid binding channel (Figure 1). Enzymatic characterization of the purified mutant agreed with in cell studies by showing decreased k_{cat} values.[19] In this earlier study we detected no change in cofactor affinity for the P133R mutant. We have now conducted in depth kinetic characterizations of the wild-type (WT) and the P133R mutant enzymes to pinpoint the molecular basis of the defective P133R enzyme. Our transient kinetic analysis revealed that the P133R mutation significantly reduced the rate of the chemical step (k_{chem}). Remarkably, the mutation drastically reduced the affinity for the NADP(H) cofactors without a comparable effect on the K_d value for steroids even though the P133R mutation is next to the steroid binding pocket and distal to the cofactor binding pocket. The reduced ability to carry out hydride transfer and decreased cofactor affinity leading to enzyme instability was identified to be the molecular defects of the mutant enzyme that may contribute to bile acid deficiency. We provide an explanation as to why this difference in cofactor affinity was not detected in our earlier study.

EXPERIMENTAL PROCEDURES

Materials

Cortisone and 7α-hydroxycholest-4-en-3-one were purchased from Steraloids. Finasteride was purchased from Sigma-Aldrich. NADPH was purchased from EMD. $NADP^+$ was purchased from Roche Applied Science. *E. coli* strain C41 (DE3) was provided by Dr. J. E. Walker (Medical Research Council Laboratory of Molecular Biology, Cambridge, UK). HisTrap Fast Flow column (5 mL) and HiTrap Blue HP column (5 mL) were purchased

from GE Healthcare. All other reagents were of American Chemical Society quality or higher.

Protein Expression and Purification

Homogenous recombinant WT AKR1D1 and the P133R mutant were expressed and purified according to published protocols with some modifications.[18] Briefly, pET28a-6His-AKR1D1 was used to overexpress both proteins in *E. coli* C41(DE3) cells upon isopropyl 1-thio-β-D-galactopyranoside induction. The harvested cells were lysed by sonication, and the protein in the soluble fraction was purified using a Zn charged HisTrap Fast Flow column (5 mL) eluted with Buffer A (20 mM Tris, pH 7.9 buffer containing 60 mM imidazole and 500 mM NaCl). The pooled fractions containing AKR1D1 were dialyzed into Buffer B (10 mM potassium phosphate buffer, pH 7.0, 1 mM 2-mercaptoethanol, 1 mM EDTA) and applied to a HiTrap Blue HP column (5 mL). The column was washed with a linear gradient of 0–1 M KCl in Buffer B. The final protein was eluted at 1 M KCl. The protein was dialyzed into 20 mM potassium phosphate buffer (pH 7.0) containing 1 mM EDTA and 30% glycerol. The purity of the final protein was assessed using SDS-PAGE, and the protein concentration was determined by Bradford protein assay using BSA as a standard (Thermo-Scientific Product #23209) 2 mg/mL in 0.9% NaCl with sodium azide.

Steady-State Kinetic Analysis

Initial velocities under steady state conditions were monitored by measuring NADPH consumption using a Hitachi F-4500 fluorescence spectrophotometer ($\lambda_{excitation}$ = 340 nm, $\lambda_{emission}$ = 460 nm). Reaction mixtures contained 0.8–65 μM cortisone or 0.4–45 μM 7α-hydroxycholest-4-en-3-one, 7.2 μM NADPH, and 4% acetonitrile in 10 mM or 100 mM potassium phosphate buffer (KPi, pH 7.0) in a total volume of 1 mL. Nonenzymatic reaction rates were determined by monitoring each sample for 3 min. Reactions were initiated by the addition of 0.09–0.3 μM AKR1D1 and followed for 3 min at 37 °C. Knowing that AKR1D1 catalyzes an ordered bi bi reaction where NADPH binds first,[20,21] the initial rates for steroid reduction were fit to the Michaelis–Menten equation or the following equation when substrate inhibition was observed:

$$v = \frac{V_{\max}[S]}{K_{\mathrm{m}} + [S] + [S]^2/K_i} \quad (1)$$

where K_i is the dissociation constant for substrate from the E-NADP$^+$ complex. The program GraFit (Erithacus Software) was used to determine the kinetic constants and are reported as mean ± SE of the mean.

Transient State Kinetic Analysis

The kinetic transients of multiple turnover reactions were monitored using an Applied Photophysics SX.19 MV stopped-flow spectrophotometer (Leatherhead, UK). Changes in the fluorescence signal of NADPH ($\lambda_{excitation}$ = 340 nm, $\lambda_{emission}$ = 450 nm) were followed upon rapid mixing of equal volumes of the premixed enzyme-cofactor solution from one syringe and the steroid solution from a second syringe. The enzyme-cofactor solution contained a fixed concentration of AKR1D1 (5 μM) and excess NADPH (35 μM), and the

steroid solution contained 50 μM of cortisone or 7α-hydroxycholest-4-en-3-one. Both solutions were in 10 mM potassium phosphate buffer (pH 7.0) containing 4% acetonitrile and were maintained at 37 °C. For each steroid substrate, the averaged reaction traces from at least three replicates were fitted to either the linear (eq 2) or the "burst" eqs (eq 3), where k_{ss} is the second-order rate constant of the linear steady-state phase, and k_{burst} is the pseudo first-order rate constant of the exponential phase.

$$y = k_{ss}[E]t + a \quad (2)$$

$$y = A\exp(-k_{burst}t) + k_{ss}[E]t + a \quad (3)$$

Intrinsic Protein Fluorescence and Energy Transfer

The intrinsic protein fluorescence of WT AKR1D1 and P133R was measured at 340 nm upon excitation at 290 nm by the addition of incremental amounts of protein (0–0.12 μM) in 10 mM potassium phosphate buffer (pH 7.0) containing 4% acetonitrile at 37 °C. The emission at 340 nm can be titrated by the addition of cofactor to measure cofactor binding affinity, while the formation of the E·NAD(P)H complex generates an energy transfer band at 460 nm, which can be quenched by the addition of steroid to measure steroid binding affinity (see below).

Cofactor Binding

The dissociation constants (K_d) for the cofactors NADPH, $NADP^+$, and NADH were determined by monitoring the quenching of protein intrinsic fluorescence upon cofactor binding as previously described ($\lambda_{excitation}$ = 290 nm, $\lambda_{emission}$ = 340 nm).[20] Briefly, incremental amounts of cofactor were added to 0.05 μM of AKR1D1 until saturation of the enzyme. The titration was performed in 10 mM or 100 mM potassium phosphate buffer (pH 7.0) containing 4% acetonitrile at 37 °C. The data were plotted as a percent change in fluorescence at 340 nm versus cofactor concentration. The data were fit to the Morrison equation using the program GraFit (Erithacus Software) (eq 4b)[22] to determine the dissociation constant.[22]

$$\Delta F/\Delta F_{max} = [R \cdot L]/[R] \quad (4a)$$

$$[R \cdot L] = [(K_d + [R] + [L]) - [(K_d + [R] + [L])^2 - 4[R][L]]^{1/2}]/2 \quad (4b)$$

ΔF is the difference in fluorescence emission in the absence and presence of ligand. ΔF_{max} is the maximum value of ΔF at saturating ligand concentration. [R·L] is the concentration of the receptor–ligand complex, [R] is the total concentration of the receptor, [L] is the total concentration of the added ligand, and K_d is the apparent dissociation constant of the ligand. In this treatment, receptor R is enzyme, ligand L is cofactor, and R·L is the enzyme-cofactor binary complex.

Ligand Chase Experiment of Cofactor—Using the stopped-flow instrument, the dissociation rate constant of $NADP^+$ from the E·$NADP^+$ complex can be determined by monitoring changes in the fluorescence energy transfer band when NADPH displaces $NADP^+$ from the cofactor binding site ($\lambda_{excitation}$ = 290 nm, $\lambda_{emission}$ = 460 nm). An enzyme-$NADP^+$ solution (AKR1D1, 1 μM; $NADP^+$, 5 μM) from one syringe was rapidly mixed (1:1) with a NADPH solution (100 μM) from the second syringe in the stopped-flow. In the control experiments, the enzyme solution or the buffer were mixed with the NADPH solution in the stopped-flow. The experiments were performed in either 10 mM or 100 mM potassium phosphate buffer (pH 7.0) containing 4% acetonitrile at 37 °C. For each condition, data from at least five replicates were averaged and fitted to either single- (eq 5a) or double-exponential eqs (eq 5b), where y is the fluorescence signal, A, A_1, and A_2 are the amplitudes, a is the intercept, and k_{obs}, k_{obs1}, and k_{obs2} are the apparent rate constants.

$$y = A\exp(-k_{obs}t) + a \quad (5a)$$

$$y = A_1\exp(-k_{obs1}t) + A_2\exp(-k_{obs2}t) + a \quad (5b)$$

Steroid Binding

The dissociation constants (K_d) for the steroids were determined by monitoring the quenching of the energy transfer band of the E·NADPH complex upon steroid binding at 460 nm ($\lambda_{excitation}$ = 290 nm, $\lambda_{emission}$ = 460 nm). An incremental amount of steroid was added to the mixture containing 0.2 μM AKR1D1 and 8 μM NADPH in 100 mM potassium phosphate buffer (pH 7.0) containing 4% acetonitrile until saturation was observed or the steroid solubility limit was reached (80 μM). The effective concentration of the E·NADPH complex was deduced based on the K_d value of the cofactor and was used for the calculation of the steroid dissociation constants. Three steroids were used in the experiment, including two substrates, cortisone and 7α-hydroxycholest-4-en-3-one, and one AKR1D1 competitive inhibitor finasteride.[23] When the substrates were used in the assay, the assay mixture was kept at 6 °C or lower to minimize turnover. When the inhibitor was used, the assay was performed at 37 °C. The data were plotted as a percent change in fluorescence at 460 nm versus steroid concentration and fit to the Morrison equation (eq 4)[22] in which R is enzyme-cofactor complex, ligand L is steroid, and R·L is the enzyme–cofactor–steroid ternary complex. When the experiment was replicated with the P133R mutant the enzyme was not fully saturated with NADPH. In this instance the fractional occupancy of the mutant by NADPH was taken into account when estimating the K_d for steroid ligand. Here the effective concentration of the P133R·NADPH complex was calculated based on the K_d of the cofactor for the mutant and the concentration of P133R used in the experiment using eq 4b.

RESULTS

The molecular defect of the P133R mutant was probed using two AKR1D1 substrates. Cortisone is a glucocorticoid mainly catabolized by 5β-reduction in the liver and is a

representative steroid hormone substrate. 7α-Hydroxycholest-4-en-3-one is the bile acid precursor for chenodeoxycholic acid, which needs 5β-reduction for maturation. The kinetic analysis was conducted assuming that the P133R mutant catalyzes an ordered bi bi kinetic mechanism in which cofactor binding is obligatory before steroid substrate binds, which is a characteristic feature of all AKRs and AKR1D1.[20,21]

Steady-State Kinetic Constants

Steady-state kinetic constants of the WT and the P133R AKR1D1 were first determined under physiologically relevant conditions of 100 mM potassium phosphate buffer (pH 7) at 37 °C. The cofactor concentration was fixed at the highest concentration permitted by the fluorimeter without eliciting an inner filter effect (7.2 μM). This concentration that allowed the WT enzyme but not the P133R mutant to be saturated by the mutant (see Cofactor Binding section for K_d). The WT enzyme showed K_m values in the low or submicromolar range with weak substrate inhibition ($K_i > 10K_m$) for both cortisone and 7α-hydroxycholest-4-en-3-one (Table 1). Cortisone is classified as a fast substrate due to its favorable k_{cat}[21] but had slightly lower catalytic efficiency (k_{cat}/K_m) than 7α-hydroxycholest-4-en-3-one due to its higher K_m. The P133R mutation reduced catalytic efficiency by affecting different kinetic constants depending on the substrate. Cortisone reduction was affected mainly by an increase in K_m, which was increased 15-fold over that seen with WT and substrate inhibition was eliminated. Saturation kinetics could not be achieved for this reaction due to the poor solubility of cortisone. The catalytic efficiency was therefore obtained from the slope of the linear portion of the initial velocity versus substrate plot (where $v/[S] = V_{max}/K_m$). Overall a 69-fold decrease in the catalytic efficiency was observed by the P133R mutant for cortisone reduction compared to the WT enzyme. 7α-Hydroxycholest-4-en-3-one reduction was affected mainly by a decrease in k_{cat}; this substrate is classified as a slow substrate due to its unfavorable k_{cat}.[21] The P133R mutant showed a 6-fold decrease in k_{cat} but maintained a low micromolar K_m for 7α-hydroxycholest-4-en-3-one resulting in a 13-fold decrease in the catalytic efficiency for the mutant compared to the WT. The effect of the P133R mutation was thus more prominent on cortisone than on 7α-hydroxycholest-4-en-3-one reduction.

The steady-state assays were also replicated in 10 mM potassium phosphate buffer. This buffer condition provides lower ionic strength and greatly decreases cofactor K_d. Saturation of the P133R mutant can now be achieved by the cofactor concentration used in initial velocity studies performed in 100 mM potassium phosphate. The impact of the P133R mutant on the apparent kinetic constants resembled the trend observed at 100 mM buffer. The steady state kinetic constants determined at subsaturating NADPH concentrations at 100 mM potassium phosphate likely reflect the values of physiological significance.

Multiple Turnover Reactions

Substrate turnover was monitored under pre-steady-state conditions using a stopped-flow instrument. Experiments were performed in 10 mM potassium phosphate buffer to allow both WT and the P133R mutant to be both saturated by the cofactor. With the WT AKR1D1, cortisone exhibited characteristic burst-phase kinetics with an initial exponential decay followed by a linear phase (Figure 2A, Table 2). The burst-phase progress curve

indicates that the reaction proceeds through a fast chemistry step (k_{burst} of 0.44 s^{-1}) where the steroid is reduced and then slows down due to the presence of a subsequent rate-limiting product release step which dictates the rate observed in the steady-state. Thus, the k_{ss} of the linear phase for cortisone reduction of 0.048 s^{-1} was consistent with the k_{cat} value of 0.053 s^{-1}. The progress curves of the multiple turnover of 7α-hydroxycholest-4-en-3-one were best fitted using the burst equation as well with a k_{burst} of 0.11 s^{-1}. However, the burst phase only accounted for 7% of the decay, suggesting more comparable rates for the chemistry step and the product release steps (k_{ss} of 0.01 s^{-1}). In contrast to WT AKR1D1, the P133R mutant exhibited linear progress curves for both cortisone and 7α-hydroxycholest-4-en-3-one reduction, indicating the rate of the chemistry step was much slower or equal to the rate of product release (Figure 2B). Data analyses yielded k_{ss} values of 0.04 s^{-1} and 0.004 s^{-1}, respectively for cortisone and 7α-hydroxycholest-4-en-3-one reduction (Table 2). In burst kinetics, the rate of the chemistry step k_{chem} is represented by k_{burst}, whereas in linear multiple turnover kinetics, k_{chem} approaches k_{ss}. Thus, the P133R mutation caused dramatic decreases in k_{chem}, over 11-fold for cortisone and over 27-fold for 7α-hydroxycholest-4-en-3-one reduction.

Intrinsic Protein Fluorescence

AKR1D1 generates intrinsic protein fluorescence at 340 nm when excited at 290 nm. This protein fluorescence is quenched upon binding of either the reduced cofactor NADPH or the oxidized cofactor $NADP^+$. Formation of the E·NADPH complex will also generate an energy transfer band at 460 mm, which is quenched upon steroid binding. The protein fluorescence of apo WT AKR1D1 and the P133R mutant and the energy transfer fluorescence of the E·NADPH complex were examined. The WT enzyme emitted a higher fluorescence signal per unit of protein than the P133R mutant ($\lambda_{excitation}$ = 290 nm, $\lambda_{emission}$ = 340 nm) but a similar energy transfer band per unit of NADPH ($\lambda_{excitation}$ = 290 nm, $\lambda_{emission}$ = 460 nm) (Figure 3). Protein fluorescence is heavily affected by solvent-tryptophan interaction. AKR1D1 contains five tryptophan residues at positions 89, 140, 151, 230, and 314. On the basis of homology to rat 3α-hydroxysteroid dehydrogenase (AKR1C9).[24,25] Trp151 is predicted to be a major contributor to the intrinsic protein fluorescence, and Trp89 is responsible for energy transfer band in the E·NADPH complex. A change in intrinsic protein fluorescence indicates the P133R mutation elicited a structural change and affected the environment of the tryptophan residues. But the undisturbed energy transfer band suggested that Trp89, which sits deeply in the steroid binding channel, was not perturbed in its environment.

Cofactor Binding

Cofactor binding affinity was assessed by determining dissociation constants (K_d) by titration and by measuring the rate of $NADP^+$ release rate (k_{off}) under transient kinetic conditions. The K_d measurements took advantage of the quenching of the AKR1D1 intrinsic fluorescence upon cofactor binding. Under physiological conditions (100 mM potassium phosphate buffer, pH 7.0), WT AKR1D1 binds both cofactors NADPH and $NADP^+$ tightly with submicromolar K_d values (~0.3 μM) (Table 3). The P133R mutant dramatically lowered the cofactor binding affinity by increasing the K_d values over 40-fold to reach the 20 μM range.

A reduction in ionic strength from 100 mM to 10 mM potassium phosphate buffer significantly increased cofactor affinity. This is likely due to stronger interaction between Arg279 and the phosphate group of the cofactor in the absence of competing buffer ions.[26] The K_d values for both the WT enzyme and the P133R mutant were decreased in 10 mM potassium phosphate to the low nanomolar range but demonstrated a similar fold change (Table 3). As a result, K_{dNADPH} for the P133R mutant (0.075 μM) remained 30-fold higher than the K_{dNADPH} value for the WT enzyme (0.0023 μM). The P133R $K_{d,NADPH}$ of 0.075 μM is essentially identical to that reported in our previous characterization of this mutant.[19] In that earlier study, we reported that this value was no different from WT AKR1D1. The difference in cofactor affinity between WT AKR1D1 and P133R now observed was not detected in our earlier work because we isolated both WT AKR1D1 and P133R using only Ni-Sepharose affinity column chromatography. This resulted in a significant portion of the WT AKR1D1 being isolated in the $NADP^+$ bound form due to its very high affinity for this cofactor K_d = 4.3 nM. In the present study, only enzyme that was subsequently purified on Blue-Sepharose was used, ensuring that both enzyme forms were cofactor free.

In our earlier work, we had reported that the intrinsic protein fluorescence observed for P133R versus WT AKR1D1 was 5 times greater, when in fact we now find that WT AKR1D1 has 1.5 times the intrinsic fluorescence of P133R (see Figure 3A). We attribute this difference due to WT.AKR1D1 in the earlier work being in the cofactor bound form. In the earlier work the intrinsic protein fluorescence was less for WT AKR1D1 indicative of Trp quenching by bound cofactor; however, no energy transfer band was present, suggesting that the form of cofactor bound was $NADP^+$. Using the correct K_{dNADP+} for WT AKR1D1 we estimate that from previous cofactor titrations that 90% of the enzyme was in the cofactor bound form. It is noteworthy that T_m curves obtained by CD spectroscopy for WT AKR1D1 and the P133R mutant yielded values of 49 and 41 °C, respectively. However, when NADPH was added the T_m curves were superimposable with values of 50–51 °C. These data also support that WT AKR1D1 purified by Ni-Sepharose chromatography was most likey in the more stable $NADP^+$ bound form.

To validate the difference in cofactor affinity between WTAKRD1 and P133R the rate of $NADP^+$ release k_{off} was measured by following the formation of the energy transfer band by chasing $NADP^+$ from the E·$NADP^+$ complex with NADPH. Control experiments were performed to ensure the NADPH on-rate is not the rate-limiting step during the cofactor exchange. In 100 mM phosphate buffer, WT AKR1D1 exhibited a single-exponential trace for $NADP^+$ release, which could be best fitted to an equation to yield a k_{off}^{WT} of 0.28 s^{-1}. In contrast, the P133R mutant caused a striking increase in the $NADP^+$ release rate, which was too fast to be captured by the instrument (instrument dead time ~1.8 ms, $k_{off}^{P133R} > 50\ s^{-1}$) (Figure 4, Table 4). The amplitude of the fluorescence signal of the mutant was about one-half of that observed with the WT enzyme. This can be explained by the increase in K_d, which dictates that a significant portion of the mutant enzyme will not be in the binary form compared to the WT.

Even though 10 mM potassium phosphate is not physiologically relevant, this condition allowed us to probe the effect of the P133R mutant on cofactor binding more readily since the mutant could be saturated by the cofactor in a concentration range that could be tolerated

by the stopped-flow instrument. Thus, the chase experiments were repeated in 10 mM buffer. WT AKR1D1 yielded a similar single-exponential chase curve with a k_{off}^{WT} of 0.164 s^{-1}. This rate is 3-fold less than k_{burst} observed for cortisone reduction under multiple turnover conditions and would account for the observed burst phase kinetics. This value is also similar to k_{burst} 0.11 s^{-1} of 7α-hydroxycholest-4-en-3-one, but higher than k_{ss}, suggesting for this substrate, steroid product release must also contribute to overall rate determination. Using eq 6,[27] the rate of steroid product release can be estimated, where k_{chem} is the rate of the chemistry step represented by k_{burst} of 0.11 s^{-1} and $k_{r,NADP^+}$ is the release of $NADP^+$ of 0.164 s^{-1}. From this equation the steroid release rate $k_{r,Sp}$ for 7α-hydroxycholest-4-en-3-one is estimated to be 0.02 s^{-1}, which is comparable to the k_{ss} value.

$$(1/k_{cat})=(1/k_{chem})+(1/k_{r,Sp})+(1/k_{r,NADP^+}) \quad (6)$$

By conducting the chase experiments in 10 mM potassium phosphate we found that the P133R mutant also generated a single-exponential chase curve with a measurable k_{off}^{P133R} of 8.9 s^{-1}, which is 54-fold higher than the cofactor release rate of 0.164 s^{-1} for the wild-type enzyme.

The dissociation constant for the less favored cofactor NADH was also determined. Unlike NADPH, K_d values of NADH were not affected by ionic strength or the P133R mutation. Both WT and the P133R mutant gave high K_d values around 30 μM due to the lack of the interaction between the 2′-AMP phosphate and Arg 279.

Steroid Binding

Steroid binding was assessed by measuring the dissociation constants (K_d) by titrating the energy transfer band of the E·NADPH complex. Two steroid substrates, cortisone and 7α-hydroxycholest-4-en-3-one, and one competitive inhibitor of AKR1D1, finasteride, were used. K_d for the steroid substrates was determined at low temperature to minimize turnover. The K_d for the inhibitor finasteride was determined at a normal assay temperature of 37 °C to demonstrate that the difference in temperature had little effect on the observed differences in K_d. WT AKR1D1 exhibited similar K_d values in low micromolar range for all three steroid ligands despite the difference in temperature (Table 5). Cortisone showed tighter binding affinity than 7α-hydroxycholest-4-en-3-one yielding a 4-fold reduction in K_d. The P133R mutant also showed similar binding affinity for all three ligands, but their K_d values were now 4–10 fold higher than the corresponding K_d values of the WT. For the P133R mutant, the K_d values for steroid were calculated after correcting for partial occupancy of the mutant with NADPH. K_d values may also be an underestimate of the true values in this instance due to the inability to achieve saturation at the limit of steroid solubility.

DISCUSSION

Mutations in AKR1D1 are the second leading cause of primary bile acid deficiency following defects in 3β-hydroxy-Δ^5-C_{27}-steroid oxidoreductase.[28,29] Seven point mutations have been identified in patients with AKR1D1 deficiency, and we have characterized five of them *in vitro* (L106F, P133R, P198L, G223E, R261C).[19] However, how these mutations

affect protein stability and enzyme activity has not been fully elucidated. In this report we focused on the purified recombinant P133R mutant and dissect its effects on two substrates, cortisone, a steroid hormone, and 7α-hydroxycholest-4-ene-3-one, a principal primary bile acid precursor.

We find that the P133R mutation decreases the catalytic efficiency (k_{cat}/K_m) of the enzyme by 13–69 fold. This effect was greater with the smaller C_{21} steroid cortisone or fast substrates (69-fold) than with the C_{27} bile acid precursor 7α-hydroxycholest-4-ene-3-one or slow substrates (13-fold). The reduction in catalytic efficiency observed with cortisone was primarily caused by an increase on K_m. A similar finding was observed when the P133R mutant was transiently transfected into HEK293 cells, where 5β-reduction of small C_{19} steroid testosterone was mainly affected by K_m.[19] The steroid binding channel is formed by the three long flexible loops, A (Ile119-Leu147), B (Tyr219-Leu238), and C (Leu302-Tyr326). Proline usually provides rigidity to the structure, and the introduction of the P133R mutation likely affects loop A and hence the conformation of the steroid channel, causing an increase in steroid K_d.

The reduction in catalytic efficiency seen with 7α-hydroxycholest-4en-3-one in the P133R mutant was prirmarily due to changes in k_{cat}. This C27 steroid has a more extensive side-chain which can provide additional interactions between the steroid and the enzyme which results in a lower K_m in the WT enzyme.[30] A docking study of 7α-hydroxycholest-4-en-3-one to WT AKR1D1 indicates that the C17 side chain extends out of the steroid channel and binds in the grooves formed by loops B and C on the surface of the enzyme.[30] The P133R mutant appears to influence the steroid binding channel but does not disrupt this additional interaction. Thus, the mutant has a larger impact on the K_d for cortisone than on the K_d for 7α-hydroxycholest-4-en-3-one and finasteride.

To understand the impact of the P133R mutant on the rate of the chemical step (k_{chem}) transient kinetics were performed under multiple turnover conditions for both substrates. The WT enzyme shows burst phase kinetics for both cortisone and 7α-hydroxycholest-4en-3-one, indicating a fast chemical step followed by a rate limiting product release step. With the mutant, k_{chem} was reduced by 10-fold for cortisone but by 30-fold for 7α-hydroxycholest-4-en-3-one and becomes the major rate-limiting step for both substrates, as indicated by the linear progression curves. Structural perturbations of enzyme can dramatically alter the rates of the reaction, even when these alterations are distant from the active site.[31] For example, mutations in the nonactive site residue Cys191 in aspartate aminotransferase reduces enzyme activity by disrupting the hydrogen bonding to its adjacent loop, which is required for pyridoxal phosphate binding.[32] Similarly, the G121V mutation in dihydrofolate reductase decreases the rate of the hydride transfer step by 200-fold, by affecting the rate of conformation changes during catalysis.[31] If it is considered that an enzyme exists in a population of different conformations to facilitate different microreaction steps, e.g., substrate binding, orienting, and optimizing the electrostatic environment, a nonactive site mutation may cripple the reaction by inducing a suboptimal distribution of different conformations or even favoring a nonproductive conformation.[33]

Steroid 5β-reduction catalyzed by AKR1D1 undergoes several conformational changes especially during cofactor binding. Similar to the other related enzymes AKR1C9 and AKR1C2[20,34] the cofactor binding of AKR1D1 involves a fast step to form an initial loose complex followed by slow isomerization steps to form the final tight complex.[21] Even though the P133R residue is located closer to the steroid binding site than the cofactor binding site in structure, our data demonstrate a surprising finding that the P133R mutation drastically decreases cofactor binding affinity. The mutant increases the K_d for NADP(H) by 20–100 fold and increases the rate of release of $NADP^+$ release by over 50 fold. The P133R mutation likely affects the isomerization step during cofactor binding, which results in a preference for the loose complex. This could reduce k_{chem} by two mechanisms: one is to reduce the rate of conformational change to produce the tight complex, and the other is to disrupt the trajectory of hydride transfer. The chemistry step of 5β-reduction is comprised of the hydride transfer step and the proton donation step. Hydride transfer is very sensitive to donor–receptor distance and alignment.[35] By favoring the formation of the loose complex, the mutant allows the cofactor to wobble in the binding site, interrupting hydride transfer and lowering k_{chem}.

Importantly the binding of NADH was not affected by the P133R mutant, indicating the mutant affects the interaction of Arg279 with the 2′-phosphate of AMP in the cofactor. This salt linkage is required for the tight binding of NADPH.[26] The intrinsic protein fluorescence is greater for the WT enzyme than the P133R, but the amplitude of the energy transfer band when binding cofactor remains unchanged. Quenching of Trp89 is likely responsible for the energy transfer band based on homology with AKR1C9[25] and is unaffected by the P133R mutant. These data show that despite the lower affinity of NADPH for the P133R mutant this is not reflected in a weaker interaction between the nicotinamide headgroup of the cofactor and Trp 89. The remaining tryptophan residues in AKR1D1 are located in the loops that form the ligand binding sites except Trp 151. We hypothesize that the P133R mutation changes the loop conformation/flexibility and thus disrupts the hydrogen network between the loops. This has a long-range effect on the cofactor binding loop and the interaction with Arg279. This effect of the P133R mutant will be exacerbated *in vivo*, since cofactor affinity determines cofactor occupancy of the enzyme in the cell. The strikingly high K_d of the P133R mutation for NADP(H) suggests that the mutant enzyme will be mostly cofactor free *in vivo* and be more labile.[18] Thus, the effect of the P133R mutant is to reduce cofactor binding, reduce k_{chem}, and make the protein more unstable.

Acknowledgments

Funding

This work was supported by grants from the National Institutes of Health as follows: P30-ES013508 and R01-DK47015 (awarded to T.M.P.); by F32-DK-089827 to M.C.; and a pilot project from P30-ES013508 to Y.J.

ABBREVIATIONS

AKR	aldo-keto reductase
AKR1D1	Δ^4-3-ketosteroid 5β-reductase

CYP7A1	gene for cytochrome P4507A1
FXR	farnesoid X receptor
T_m	melting temperature obtained by CD spectroscopy
WT	wild type

References

1. Russell DW. The enzymes, regulation, and genetics of bile acid synthesis. Annu Rev Biochem. 2003; 72:137–174. [PubMed: 12543708]
2. Lefebvre P, Cariou B, Lien F, Kuipers F, Staels B. Role of bile acids and bile acid receptors in metabolic regulation. Physiol Rev. 2009; 89:147–191. [PubMed: 19126757]
3. Clayton PT, Patel E, Lawson AM, Carruthers RA, Tanner MS, Strandvik B, Egestad B, Sjövall J. 3-Oxo-Δ^4 bile acids in liver disease. Lancet. 1988; 331:1283–1284. [PubMed: 2897546]
4. Callachan H, Cottrell GA, Hather NY, Lambert JJ, Nooney JM, Peters JA. Modulation of the $GABA_A$ receptor by progesterone metabolites. Proc R Soc London, Ser B. 1987; 231:359–369. [PubMed: 2888123]
5. Sheehan PM, Rice GE, Moses EK, Brennecke SP. 5b-Dihydroprogesterone and steroid 5b-reductase decrease in association with human parturition at term. Mol Hum Reprod. 2005; 11:495–501. [PubMed: 16123077]
6. Levere RD, Kappas A, Granick S. Stimulation of hemoglobin synthesis in chick blastoderms by certain 5b-androstane and 5b-pregnane steroids. Proc Natl Acad Sci U S A. 1967; 58:985–990. [PubMed: 5233854]
7. Navarro JF. In the erythropoietin era, can we forget alternative or adjunctive therapies for renal anaemia management? The androgen example. Nephrol Dial Transplant. 2003; 18:2222–2226. [PubMed: 14551346]
8. Setchell KD, Suchy FJ, Welsh MB, Zimmer-Nechemias L, Heubi J, Balistreri WF. Δ^4-3-oxosteroid 5b-reductase deficiency described in identical twins with neonatal hepatitis. A new inborn error in bile acid synthesis. J Clin Invest. 1988; 82:2148–2157. [PubMed: 3198770]
9. Clayton PT. Disorders of bile acid synthesis. J Inherited Metab Dis. 2011; 34:593–604. [PubMed: 21229319]
10. Kimura A, Kondo KH, Okuda KI, Higashi S, Suzuki M, Kurosawa T, Tohma M, Inoue T, Nishiyori A, Yoshino M, Kato H, Setoguchi T. Diagnosis of the first Japanese patient with 3-oxo-Δ^4-steroid 5b-reductase deficiency by use of immunoblot analysis. Eur J Pediatr. 1998; 157:386–390. [PubMed: 9625335]
11. Sinal CJ, Tohkin M, Miyata M, Ward JM, Lambert G, Gonzalez FJ. Targeted disruption of the nuclear receptor FXR/BAR impairs bile-acid and lipid homeostatsis. Cell. 2000; 102:731–744. [PubMed: 11030617]
12. Palermo M, Marazzi MG, Hughes BA, Stewart PM, Clayton PT, Shackleton CH. Human Δ^4-3-oxosteroid 5beta-reductase (AKR1D1) deficiency and steroid metabolism. Steroids. 2008; 73:417–423. [PubMed: 18243262]
13. Gonzales E, Cresteil D, Baussan C, Dabadie A, Gerhardt MF, Jacquemin E. SRD5B1 (AKR1D1) gene analysis in Δ^4-3-oxosteroid 5b-reductase deficiency: evidence for primary genetic defect. J Hepatol. 2004; 40:716–718. [PubMed: 15030995]
14. Lemonde HA, Custard EJ, Bouquet J, Duran M, Overmars H, Scambler PJ, Clayton PT. Mutations in SRD5B1 (AKR1D1), the gene encoding Δ^4-3-oxosteroid 5b-reductase, in hepatitis and liver failure in infancy. Gut. 2003; 52:1494–1499. [PubMed: 12970144]
15. Ueki I, Kimura A, Chen HL, Yorifuji T, Mori J, Itoh S, Maruyama K, Ishige T, Takei H, Nittono H, Kurosawa T, Kage M, Matsuishi T. *SRD5B1* gene analysis needed for the accurate diagnosis of primary 3-oxo-Δ^4-steroid 5b-reductase deficiency. J Gastroenterol Hepatol. 2009; 24:776–785. [PubMed: 19175828]

16. Zhao J, Fang LJ, Setchell KD, Chen R, Li LT, Wang JS. Primary Δ^4-3-oxosteroid 5b-reductase deficiency: Two cases in China. World J Gastroenterol. 2012; 18:7113–7117. [PubMed: 23323017]
17. Mindnich R, Drury JE, Penning TM. The effect of disease associated point mutations on 5β-reductase (AKR1D1) enzyme function. Chem Chem-Biol Interact. 2011; 191:250–254. [PubMed: 21185810]
18. Di Costanzo L, Drury JE, Penning TM, Christianson DW. Crystal structure of human liver Δ^4-3-ketosteroid 5b-reductase (AKR1D1) and implications for substrate binding and catalysis. J Biol Chem. 2008; 283:16830–16839. [PubMed: 18407998]
19. Drury JE, Mindnich R, Penning TM. Characterization of disease-related 5b-reductase (AKR1D1) mutations reveals their potential to cause bile acid deficiency. J Biol Chem. 2010; 285:24529–24537. [PubMed: 20522910]
20. Jin Y, Penning TM. Multiple steps determine the overall rate of the reduction of 5a-dihydrotestosterone catalyzed by human type 3 3a-hydroxysteroid dehydrogenase: Implications for the elimination of androgens. Biochemistry. 2006; 45:13054–13063. [PubMed: 17059222]
21. Jin Y, Chen M, Penning TM. Rate of steroid double-bond reduction catalysed by the human steroid 5b-reductase (AKR1D1) is sensitive to steroid structure: implications for steroid metabolism and bile acid synthesis. Biochem J. 2014; 462:163–171. [PubMed: 24894951]
22. Morrison JF. Kinetics of the reversible inhibition of enzyme-catalysed reactions by tight-binding inhibitors. Biochim Biophys Acta. 1969; 185:269–286. [PubMed: 4980133]
23. Drury JE, Di Costanzo L, Penning TM, Christianson DW. Inhibition of human steroid 5b-reductase (AKR1D1) by finasteride and structure ofthe enzyme-inhibitor complex. J Biol Chem. 2009; 284:19786–19790. [PubMed: 19515843]
24. Jez JM, Bennett MJ, Schlegel BP, Lewis M, Penning TM. Compartive anatomy of the aldo-keto reductase superfamily. Biochem J. 1997; 326(Pt3):625–636. [PubMed: 9307009]
25. Jez JM, Schlegel BP, Penning TM. Characterization of the substrate binding site in rat liver 3a-hydroxysteroid/dihydrodiol dehydrogenase. J Biol Chem. 1996; 271:30190–30198. [PubMed: 8939970]
26. Ratnam K, Ma H, Penning TM. The arginine 276 anchor for NADP(H) dictates fluorescence kinetic transients in 3a-hydroxysteroid dehydrogenase, a representative aldo-keto reductase. Biochemistry. 1999; 38:7856–7864. [PubMed: 10387026]
27. Plapp BV. On calculation of rate and dissociation constants from kinetic constants for the Ordered Bi Bi mechanism of liver alcohol dehydrogenase. Arch Biochem Biophys. 1973; 156:112–114. [PubMed: 4730466]
28. Cheng JB, Jacquemin E, Gerhardt M, Nazer H, Cresteil D, Heubi JE, Setchell KDR, Russell DW. Molecular genetics of 3b-hydroxy-Δ5-C27-steroid oxidoreductase deficiency in 16 patients with loss of bile acid synthesis in liver disease. J Clin Endocrinol Metab. 2003; 88:1833–1841. [PubMed: 12679481]
29. Subramaniam P, Clayton PT, Portmann BC, Mieli-Vergani G, Hadzic N. Varaible clinical spectrum of the most common inborn error fo bile-acid metabolism 3b-hydroxy-Δ^5 C27-steroid dehydrogenase. J Pediatr Gastroenterol Nutr. 2010; 50:61–66. [PubMed: 19915491]
30. Chen M, Drury JE, Penning TM. Substrate specificity and inhibitor analyses of human steroid 5b-reductase (AKR1D1). Steroids. 2011; 76:484–490. [PubMed: 21255593]
31. Hammes GG, Benkovic SJ, Hammes-Schiffer S. Flexibility, diversity, and cooperativity: pillars of enzyme catalysis. Biochemistry. 2011; 50:10422–10430. [PubMed: 22029278]
32. Jeffery CJ, Gloss LM, Petsko GA, Ringe D. The role of residues outside the active site: structural basis for function of C191 mutants of Escherichia coli aspartate aminotransferase. Protein Eng, Des Sel. 2000; 13:105–112.
33. Bhabha G, Lee J, Ekiert DC, Gam J, Wilson IA, Dyson HJ, Benkovic SJ, Wright PE. A dynamic knockout reveals that conformational fluctuations influence the chemical step of enzyme catalysis. Science. 2011; 332:234–238. [PubMed: 21474759]
34. Cooper WC, Jin Y, Penning TM. Elucidation of a complete kinetic mechanism for a mammalian hydroxysteroid dehydrogenase (HSD) and identification of all enzyme forms on the reaction coordinate. J Biol Chem. 2007; 282:33484–33493. [PubMed: 17848571]

35. Mesecar AD, Stoddard BL, Koshland DE. Orbital steering in the catalytic power of enzymes: small structural changes with large catalytic consequences. Science. 1997; 277:202–206. [PubMed: 9211842]

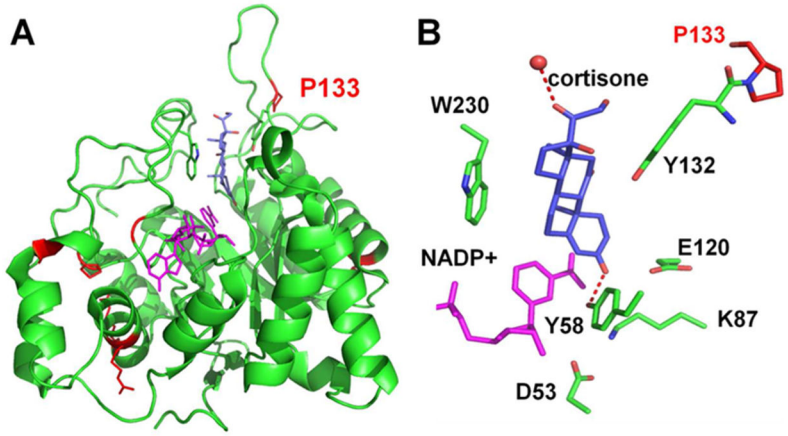

Figure 1.

Location of P133 in the crystal structure of AKR1D1 in complex with $NADP^+$ (magenta) and cortisone (blue) (PDB: 3CMF). The P133 residue (red) is located on the loop forming the steroid binding channel (A) but does not make direct contact with the steroid molecule (B). The residue is distal to the cofactor and catalytic tetrad (Asp53, Tyr58, Lys87, and Glu120). The location of other six disease-related point mutations are shown in red (A). Noncarbon atoms are color-coded as follows: oxygen, red; nitrogen, blue. Hydrogen bonds are indicated by red dashes. Figures are prepared using The PyMOL Molecular Graphics System, Version 1.20 Schrödinger, LLC.

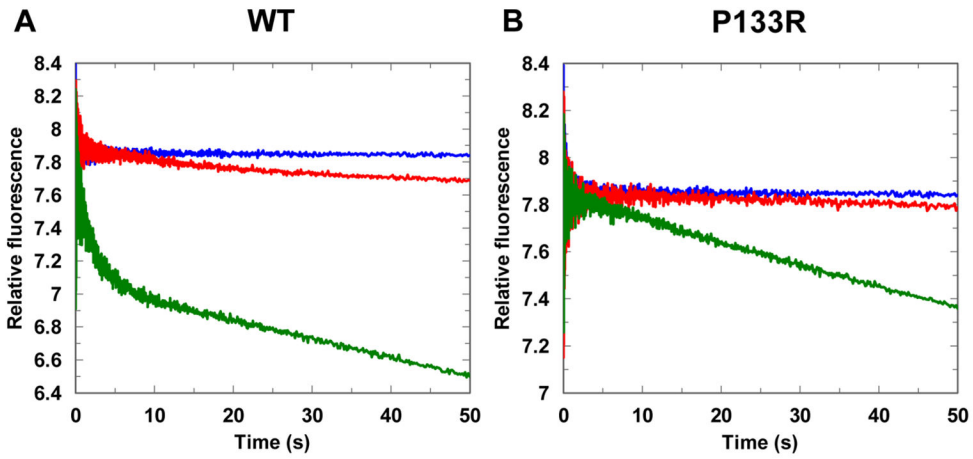

Figure 2.

Multiple turnover reactions. Representative fast substrate cortisone (green) and slow substrate 7*α*-hydroxycholest-4-en-3-one (red) showed burst kinetics with the WT (A) and linear kinetics with the P133R mutant (B). The control reaction without enzyme is in blue.

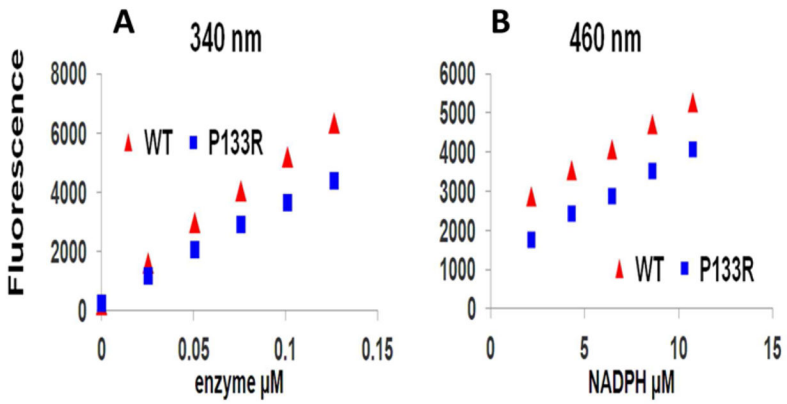

Figure 3.

Protein fluorescence. AKR1D1 has intrinsic protein emission at 340 nm when excited at 290 nm. WT (blue square) showed higher unit fluorescence then the P133R mutant (red triangle), panel A. This emission is quenched upon cofactor binding and generate an energy transfer band at 460 nm. WT (red triangle) showed similar unit energy transfer intensity to the P133R mutant (blue square), panel B.

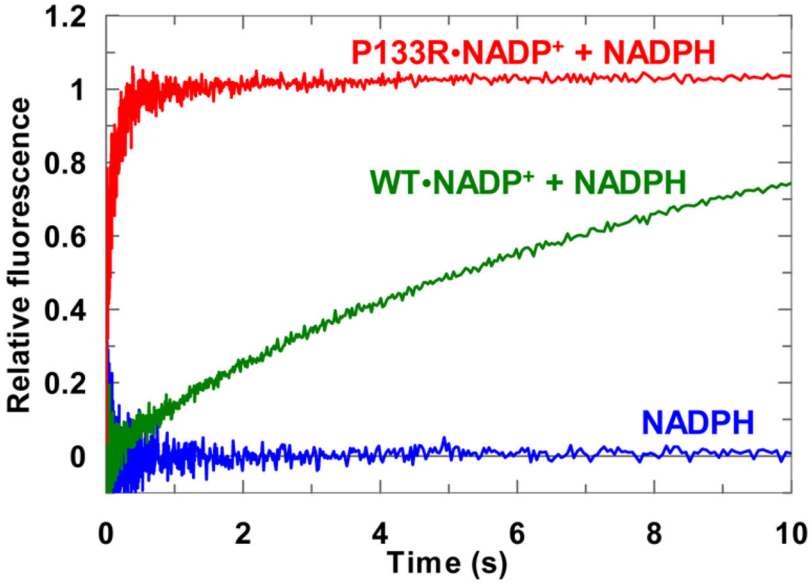

Figure 4.

Ligand chase experiments. $NADP^+$ is chased from the E·$NADP^+$ complex by NADPH. The P133R mutant (red) showed a much faster $NADP^+$ release rate than the WT (green). Experiments performed in 100 mM KPi buffer pH 7.0.

Table 1

Steady-State Kinetic Constants of the WT and the P133R AKR1D1

	cortisone		7α-hydroxycholest-4-en-3-one	
	100 mM KPi	**10 mM KPi**	**100 mM KPi**	**10 mM KPi**
WT				
k_{cat} (s^{-1})	0.103 ± 0.002	0.053 ± 0.002	0.020 ± 0.002	0.017 ± 0.001
K_m (μM)	4.1 ± 0.2	2.5 ± 0.2	0.5 ± 0.2	1.0 ± 0.2
K_i (μM)	55 ± 4	94 ± 13	46 ± 18	55 ± 14
k_{cat}/K_m (s^{-1} M^{-1})	25000	21200	40000	17000
P133R[a]				
k_{cat} (s^{-1})	>0.028[b]	>0.036[b]	0.0030 ± 0.0005 (WT/P133R 6.7)	0.0017 ± 0.0001 (WT/P133R 10)
K_m (μM)	>70[b]	>200[b]	1.0 ± 0.4 (WT/P133R 0.5)	2.4 ± 0.7 (WT/P133R 0.42)
K_i (μM)	NA	NA	51 ± 27	NA
k_{cat}/K_m (s^{-1} M^{-1})	362[b] (WT/P133R 69)	760[b] (WT/P133R 27.9)	3000 (WT/P133R 13.3)	1100 (WT/P133R 15.4)

[a] Steady-state kinetic parameters for the P133R mutant conducted in 100 mM KPi are apparent values only since it is not possible to saturate the enzyme with NADPH.

[b] P133R catalyzed cortisone reductions at 10 mM KPi or 100 mM KPi did not show saturation kinetics at the highest substrate concentration attempted. Values of k_{cat} and K_m could not be accurately determined and k_{cat}/K_m was calculated from the slope of initial rate versus substrate concentration curve.

Table 2

Transient Kinetic Rate Constants for the WT and the P133R AKR1D1

	cortisone[a]		7α-hydroxycholest-4-en-3-one[a]	
	k_{burst} (s^{-1})	k_{ss} (s^{-1})	k_{burst} (s^{-1})	k_{ss} (s^{-1})
WT	0.44 ± 0.01	0.048 ± 0.001	0.11 ± 0.02	0.010 ± 0.002
P133R	no burst	0.040 ± 0.001	no burst	0.004 ± 0.001
k_{chem} WT/P133R		11		27

[a]Assays were performed in 10 mM potassium phosphate buffer, pH 7, 37 °C.

Table 3

Cofactor Binding Constants for the WT and the P133R AKR1D1

	NADPH		$NADP^+$		NADH	
K_d (μM)	100 mM KPi	10 mM KPi	100 mM KPi	10 mM KPi	100 mM KPi	10 mM KPi
WT	0.324 ± 0.008	0.0023 ± 0.0006	0.237 ± 0.005	0.0043 ± 0.0006	34.8 ± 3.5	24.8 ± 1.7
P133R	14.5 ± 0.4	0.075 ± 0.005	27.1 ± 1.3	0.080 ± 0.006	34.5 ± 3.8	28.4 ± 1.9
P133R/WT	45	33	114	19	1	1.1

Table 4

Rates of $NADP^+$ Release from the WT and the P133R AKR1D1

	$NADP^+$ k_{off} (s^{-1})	
	100 mM KPi	**10 mM KPi**
WT	0.276 ± 0.008	0.164 ± 0.007
P133R	>50	8.9 ± 0.2
P133R/WT	>180	54

Table 5

Steroid Binding Constants for WT AKR1D1 and the P133R Mutant

K_d (μM)	cortisone[a]	7α-hydroxycholest-4-en-3-one[a]	finasteride[a]
WT	0.87 ± 0.07	2.2 ± 0.3	3.7 ± 0.2
P133R	11.1 ± 1.5	13.6 ± 1.9	14.2 ± 1.3
P133R/WT	13	6	4

[a] Assays were performed in 100 mM potassium phosphate buffer, pH 7. Assay temperature was 37 °C for inhibitor and 4 °C for substrates.